

# FINAL PUBLISHABLE JRP REPORT

JRP-Contract number	IND54	
JRP short name	Nanostrain	
JRP full title	Novel electronic devices based on control of strain at the nanoscale	
Version numbers of latest contracted Annex Ia and Annex Ib against which the assessment will be made	Annex Ia:	V1.1
	Annex Ib:	V1.01
Period covered (dates)	From 01 July 2013	To 31 June 2016
JRP-Coordinator		
Name, organisation	Mark Stewart, NPL	
Tel:	+44 208 943 8524	
Email:	mark.stewart@npl.co.uk	
Website address	<a href="http://www.piezoinstitute.com/resources/emrp-nanostrain/">http://www.piezoinstitute.com/resources/emrp-nanostrain/</a>	
Other partners		
Short name, country	BAM, Germany CMI, Czech Republic PTB, Germany ULiv, United Kingdom	
REG-Researcher (associated Home Organisation)	Martin Hýtch (CNRS, France)	Start date: 01 September 2013 Duration: 34 months
REG-Researcher (associated Home Organisation)	Jason Crain (UED, United Kingdom)	Start date: 01 January 2014 Duration: 30 months
REG-Researcher (associated Home Organisation)	Chris Lucas (ULiv, United Kingdom)	Start date: 01 March 2014 Duration: 24 months

---

**Report Status: PU Public**



**TABLE OF CONTENTS**

1	Executive summary .....	3
2	Project context, rationale and objectives.....	4
3	Research results .....	5
4	Actual and potential impact.....	22
5	Website address and contact details .....	24
6	List of publications.....	24

## 1 Executive summary

### Introduction

This project set out to develop new metrological techniques and infrastructure to aid the development of novel electronic devices with the potential to become the next generation of processors for faster, smaller and more energy efficient computing. Today's transistor technology is approaching the limit of processing power and size, so innovative solutions are being developed by global leaders in semiconductor research. One contender for the new transistor uses **strain** to control materials properties at the **nanoscale**. This project has developed new measurement tools and models to predict characterise strain at the nanoscale to aid manufacturers in the understanding and development of these novel transistors.

### The Problem

Moore's Law predicts ever increasing processing power with the doubling of transistor density every two years, however traditional scaling trends of transistor miniaturisation that accompany Moore's Law have a physical size limit predicted to occur within the next decade. Meeting the need for faster and more compact computing needed for industrial competitiveness will therefore depend on developing new transistor and memory technologies.

Amongst the raft of new technologies fighting to supersede traditional complementary metal-oxide semiconductors (CMOS) is a novel device concept based on the precise control of strain at the nanoscale using the piezoelectric effect. The application of a voltage to the piezoelectric generates strain in a piezoresistive material which in turn changes resistance, forming the transistor gate. In order to aid the design and manufacture of these devices, new characterisation and modelling tools are needed to measure and predict the strain within these materials and devices. However, there is presently no metrological framework or facilities for traceable measurement of the electro-mechanical coupling in piezoelectric materials at the required scale.

### The Solution

The project intended to support the industrial development of new functional materials inspired devices and products by developing suitable metrological techniques for strain measurement.

The solution involved the development and comparison of four different strain measurement techniques; namely X-ray diffraction, optical microscopy, transmission electron microscopy, and digital image correlation. To aid the understanding of these measurement methods and to facilitate the development of new devices, computer based modelling techniques and tools were developed to simulate behaviour at the molecular level.

### Impact

The project has led to the development of some unique and world leading facilities to characterise piezoelectric devices, which are now available for use by researchers worldwide.

- The in situ facilities at XMaS have been in high demand and resulted in many new collaborations with high profile research groups at the University of Wisconsin, and Penn State
- A new analytical capability, synchrotron-based nano-FTIR spectroscopy was established at the PTB low-energy storage ring, the Metrology Light Source (MLS), and is available for users.
- The Digital Image Correlation (DIC) expertise developed during the project is now freely available for users of the open source atomic force microscopy (AFM) analysis package Gwyddion.
- The development of ab initio modelling capabilities for the origin and control of strain in nano-scaled piezo- and ferroelectric materials, mostly at NPL, resulted in requests to access the expertise in modelling oxide films from a company developing dielectric coatings.

Based on the Nanostrain expertise two related follow on projects have been instigated, aimed at further developing piezoelectric transistor (PET) technology. PETMEM, a Horizon 2020 project, will develop PET memory and the EMPIR project 16ENG06 ADVENT will develop an RF switch for fast mobile comms. In the longer term the development of the new technologies from this project will help stimulate innovation in the microelectronics industry, with consequential economic benefits in ensuring strong European participation in the growth of the nanotechnology market. Additional environmental benefits arise from the reduced energy requirements of electronic devices using this technology, and therefore increased battery life of devices.

## 2 Project context, rationale and objectives

The European electronics sector represents 13 % of value added by total manufacturing (EC Digital Competitiveness Report 2010), but accounts for a much larger share of overall productivity growth thanks to the important role that ICT plays in boosting innovation throughout the economy. With a 25 % share of total business R&D, innovation is crucial to the future growth of this key European industry. Wider growth in nanotechnology is expected to have a major cross-sectoral impact, boosting European competitiveness and improving the lives of European citizens. Major emerging industrial applications also include ultra-high speed and resolution printing, nanoscale sensors for healthcare and industrial sensing, and power electronics.

Meeting the ever increasing need of faster computing in the ITS sector, thus securing future industrial competitiveness, depends on developing new transistor and memory technologies to extend beyond Moore's law to advance the capabilities of traditional CMOS. Moore's Law predicts ever increasing processing power with the doubling of transistor density every two years, however traditional scaling trends of transistor miniaturisation that accompany Moore's Law have a physical size limit predicted to occur within the next decade. Meeting the need for faster and more compact computing needed for industrial competitiveness will therefore depend on developing new transistor and memory technologies.

Amongst the raft of new technologies fighting to supersede traditional CMOS is a novel concept in nanoelectronic device design based on the precise control of strain within nanoscale materials using piezoelectric materials. The active part of the transistor is achieved by electro-mechanical coupling in a piezoelectric material, i.e. the generation of a strain through the application of voltage to the device.

Reliable and accurate traceable measurement of strain in new functional materials under industrially relevant conditions of high stress, electric field and at nanoscale dimensions is essential to provide the data required for new materials development, for effective design of new devices, for reliability in characterisation and testing, and to ensure quality in manufacture and reliability in service. This emerging new technology area is not currently supported by an infrastructure of traceable metrology. The expected maximum strains in thin films of piezoelectric materials are of the order of 0.1 % - 1 %. Therefore the resolution of strain measurement required is in the range of 10 ppm - 100 ppm; when this fractional change in length is to be measured on a micro-nanoscale object we find that the only currently commercially available techniques capable of performing at this level are Transmission Electron Microscopy (TEM) based methods, destructive testing techniques that are not suitable for metrology in real devices. In order to aid the design and manufacture of these devices, new characterisation and modelling tools are needed to measure and predict the strain within these materials and devices. However, there is presently no metrological framework or facilities for traceable measurement of the electro-mechanical coupling in piezoelectric materials at the required scale.

The development of suitable metrological techniques for strain measurement, and in particular non-destructive techniques that could be developed into in-line metrology at commercial volume scales, will facilitate faster development of new materials and more rapid implementation into new devices, thus providing a competitive advantage to European industry.

Although the need for beyond Moore's Law technology is largely ICT driven, there is a broader requirement across many industry sectors within Europe, spanning telecommunications, ICT, Electronics, Consumer products, instrumentation, aerospace, automotive, power, oil & gas and medical sectors. Examples of the industrial need include:-

Industry	Application	Benefit
ICT	PET application (IBM, ST Microelectronics)	Faster transistor technology, reduced power consumption
Telecoms	Smaller, faster electronic devices	Higher bandwidth, faster communications, higher mobility
Instrumentation	Manufacturers of metrology and instrumentation	Enabling more accurate measurement science
Oil and gas exploration	Novel, high accuracy sensors for secondary recovery	More efficient recovery from oil and gas wells, higher efficiencies
Aerospace and automotive	Power electronics, storage, conversion and saving.	Improved systems integration with Moore's.
Medical	Advanced MEMS/NEMS point of care diagnostics	Smaller, faster devices

Europe is particularly well positioned to benefit from new electronic components such as transistors and memory devices, based on nanoscale functional materials, with a strong technology-driven manufacturing sector and a vibrant community of innovative companies able to develop new technologies for global markets. European support for this technology would develop a market with sufficient critical mass to allow European companies to become global leaders in this field, bringing in the skills and international drivers from the project collaborators.

### **Aims and objectives**

The aims of the project were to develop the metrological infrastructure and facilities within Europe for the traceable measurement of strain in piezoelectric materials for the semiconductor industry, including production equipment and instrument manufacturers.

The first three objectives examined and compared different strain measurement techniques; namely X-ray diffraction, optical microscopy and transmission microscopy. The fourth objective sought to develop modelling on the molecular level to facilitate the development of new materials, and also to support the experimental work with simulations. The last objective looked at extending digital image correlation, not previously used for characterising piezoelectric strain, as another possible complementary strain measurement technique.

### **The specific objectives were to:**

- Develop links between traceable strain metrology and crystallographic strain via in situ interferometry and synchrotron X-ray diffraction. This enables a comparison of the intrinsic piezoelectric response (movement of atoms or ions) using X-ray diffraction, to the extrinsic response (movement and reordering of domains and grains), using interferometry.
- Develop ultra-high spatial resolution (100 nm or less) optical methods of strain measurements using infrared scanning near field microscopy (IR-SNOM) using the PTB synchrotron radiation facility (MLS) in Berlin as an IR light source.
- Develop traceable validation of macroscale strain metrology in destructive methods including Transmission Electron Microscopy (TEM) and novel holographic TEM, to map intra-grain residual and active (electric field induced) strains. A particular issue with TEM measurements are the artefacts induced during preparation, so the uncertainty caused by the additional strain from the preparation of TEM slices was also investigated.
- Develop multiphysics materials modelling to underpin all the experimental activities described above, considering both residual, process-related strains in thin film and nano/micro-scale released structures, and electrically driven strains in active devices.
- Extend the use of Digital Image Correlation processing to nano-scale functional atomic force microscopy (AFM), scanning electron microscopy (SEM) and other strain mapping images.

## **3 Research results**

### ***Objective 1: Develop links between traceable strain metrology and crystallographic strain via in situ interferometry and synchrotron X-ray diffraction.***

The overall objective here was to develop links between traceable mesoscale strain metrology and crystallographic strain via in situ interferometry and synchrotron X-ray diffraction. The key to this is the fact that many strain measurement techniques at the nano and atomistic scales describe the strain in terms of movements of atoms or groups of atoms, and X-ray diffraction is no different in this respect. X-ray diffraction measures materials in terms of unit cells of atoms and can be used to measure how these unit cells will change with the application of external stimuli such as temperature, magnetic fields, electric field etc. Whilst this gives valuable insight into the mechanisms involved in these transformations it does not necessarily describe how a more mesoscale device made up of many of these unit cells will behave in situ. The missing link here is the addition of the measurement of real world strain via in situ interferometry. The combination of an in situ interferometer with the X-ray diffractometer enables the comparison of the intrinsic piezo response, via crystallography, to its industrially highly relevant, extrinsic (domain mediated) response.

In a piezoelectric material, such as that might be used to provide the force necessary to switch a piezoresistive material in a prospective piezoelectric transistor, an applied voltage is used to effect a strain in the material. In many functional material characterisation systems for these classes of material typical measurands are the applied voltage, and the induced current or charge, since these are readily accessible and informative. A less

widely used measurand is the induced strain and or displacement, since these are more difficult to measure, particularly as the sample dimensions decrease. Commercial and laboratory made systems are available to perform these measurements. X-ray diffraction is also a common tool used to investigate functional materials and more recently researchers have applied voltages in situ to investigate the effect on piezoelectric materials. NPL and ULiv have previously added the measurement of current/charge to the in situ diffraction system at ESRF. This helps confirm that the sample is indeed seeing the applied voltage, and monitoring the current can show the sample is not changing or degrading during the experiment. In addressing the objective, the addition of an interferometer system to the beamline diffractometer brings together for the first time the simultaneous measurement of voltage, current/charge, displacement and X-ray diffraction on a piezoelectric material. This enables the measurement of in situ global strain by interferometry in comparison with the determination of the change in lattice parameters calculated from the positions of atomic reflections.

The development of the in situ capability was carried out on the XMaS beamline (BM28) at the ESRF. This is a UK EPSRC funded beamline at the ESRF in Grenoble, and was originally developed for magnetic based X-ray diffraction experiments, with 'XMaS' standing for X-ray Magnetic Scattering. More recently it has broadened its range of capabilities to include functional materials, particularly via collaborations with the NPL functional materials group. The group running the facility (ULiv) were initially an unfunded partner in the project, but were later awarded a Researcher Excellence Grant (REG) which allowed further developments to the facility.

The development of the overall in situ facility within the project was broken down into several smaller tasks:

#### ***Instrumentation development of in situ interferometry with X-ray diffraction***

The aim here was to install an interferometer on the beamline diffractometer. There were several key challenges to this task. Firstly, the environment in an experimental hutch at most synchrotron facilities is an acoustically, mechanically and electrically noisy environment, making sensitive displacement measurement very challenging. Secondly, the diffractometer itself is a difficult environment to attach an interferometer to since potentially it is moving in four different circular motions, coupled with the fact that the sample needs large angular access to the incoming and diffracted beams. Lastly, in order to develop a useable setup it is necessary to synchronise accurately the timing between the diffraction, electric polarisation and interferometry data collection as a function of the applied electric field.

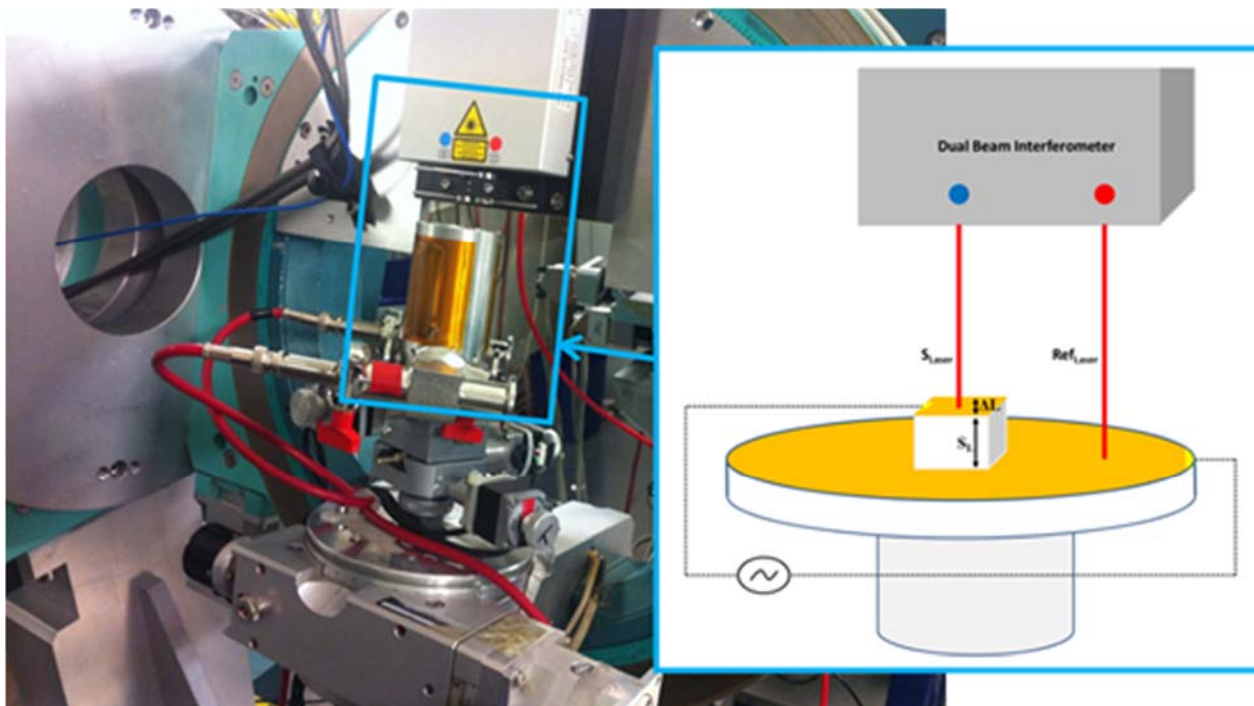


**Figure 1** Photograph of the interferometer setup on the four circle goniometer at the XMaS beamline, with a schematic of the sample setup and interferometer beam paths. The orange window is the Kapton film used to prevent unnecessary airflow but still allow the passage of the X-ray beam.

Initially the interferometer installation was to be based on a common path Jamin interferometer since NPL has many years of experience using this design, however as the design required a fibre optic delivery for the laser other options were explored. The final design chosen was a commercial Michelson system from SIOS Messtechnik GmbH. SIOS were able to deliver a cost effective solution and working with their engineers it was possible to provide a system to suit the requirements. The system is based on two parallel Michelson systems in order to remove the common path effects and SIOS added a series of lenses to enable individual control of the two interferometers to enable alignment within the confined space. The system was built in collaboration with NPL, ULiv and SIOS, and other improvements included an airtight enclosure with an angled quartz window to allow interferometer access and large Kapton windows to allow X-ray access, Figure 1. This system was designed to allow air evacuation, but was actually used to provide a controlled nitrogen atmosphere. This had two benefits: the reduction of air path movements improved the interferometer signal, and the removal of oxygen lessened the harmful effects of ozone as a result of the high intensity X-ray source. The fitted system was able to detect an AC signal of less than 50 pm on a piezoelectric single crystal, which is very challenging considering the environment.

Access to the beamline is expensive and limited, and in order to maximise usage of the facilities a parallel stand-alone 4 circle diffractometer system using a high intensity lab X-ray source was built. The standalone system is identical in almost all respects to the beamline diffractometer, apart from the flux being around three orders of magnitude smaller. This system allows the testing of the software and hardware modifications as well as giving users the ability to perform measurements and alignments prior to their allocated beamtime. This system was installed and became available for use from July 2015.

#### ***Traceable measurement of in situ strain with X-ray diffraction***

The task here was to test and characterise the in situ system developed at ESRF. The initial tests of the system focussed on large single crystals of PMN-PT, a relaxor ferroelectric material with a very large piezoelectric coefficient. The large crystal size meant that it was easier to align both the interferometer and X-rays on the same sample. One complication with the using the optical interferometer is that the sample needs to have a reasonably reflective surface for the He-Ne based laser wavelength. To achieve this, a thin gold electrode required to apply the excitation voltage was generally sufficient. Occasionally, for the transverse geometries, an extra reflective gold spot was applied. The sample also needed to be attached to a mirror surface for the reference interferometer to work from. The results from the in situ interferometer system were very encouraging. Although there are mechanical vibrations on the diffractometer in the experimental hutch causing displacement of the order of micrometres, it was possible to reduce the errors to much less than this as a result of using two collinear interferometers in order to reduce the common mode noise. The rigidity of the mounting of the interferometer and sample meant that it was possible to maintain alignment even though the system was turned upside down as a consequence of the diffraction angle. Some allowance was made for settling after each motor move, as the step-stop movements induced a short ringing vibration in process. Overall these tests showed an excellent agreement between the measurements made using the interferometer and the results of the diffraction, with an almost perfect 1 to 1 correspondence, Figure 2.

This is not entirely unexpected since the sample was a single crystal and the domain related motions are likely to be less than expected in more polycrystalline samples. However it should be noted that the interferometer strain is a result of the entire sample motion, in this case 4mm, whereas the X-ray diffraction signal comes from a thin region of 10s of micrometres near the sample surface. This work was written up and published as a peer reviewed paper in Review of Scientific Instruments.

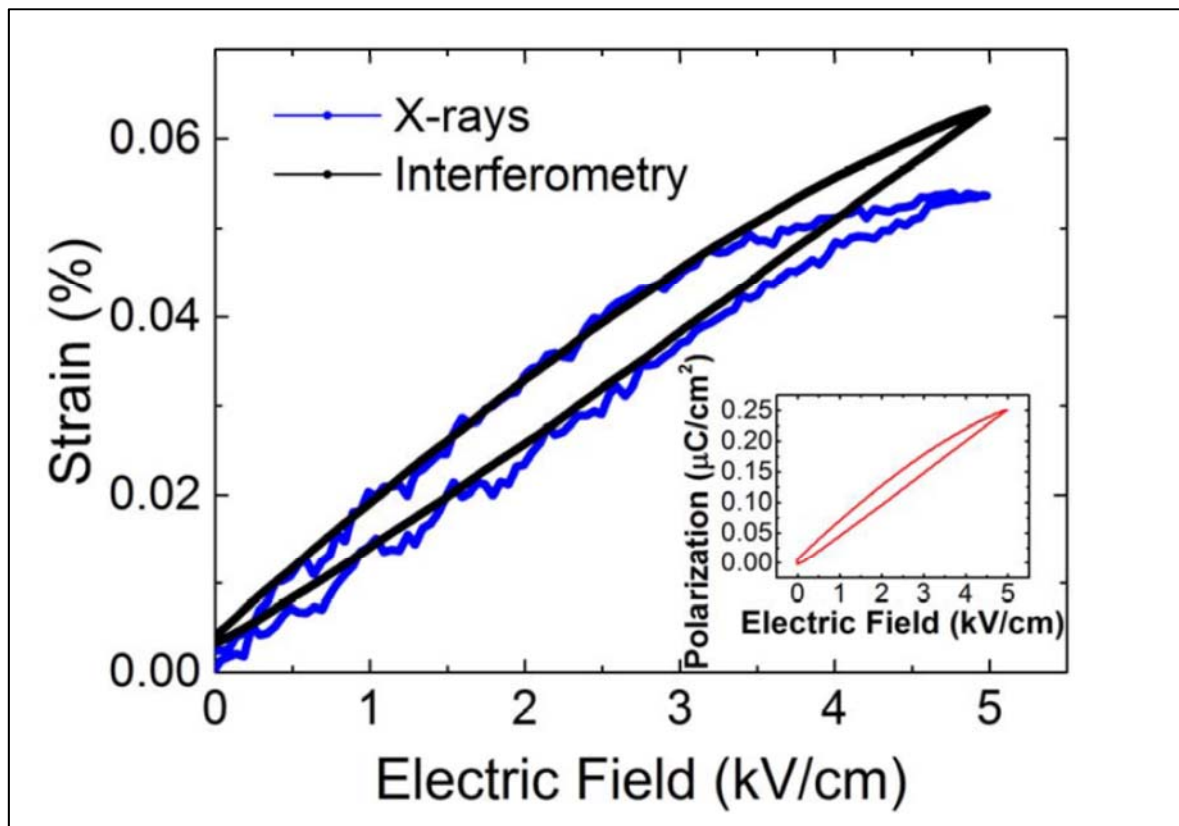


**Figure 2** Strain dependence as function of applied ac (frequency = 1 Hz) Electric field of a PMN-PT single crystal on the (0 0 2) specular reflection. Blue line shows the lattice (from X-ray data) intrinsic contribution, the black line represents the strain as measured by the laser interferometer. Inset: the red line represents the simultaneously measured electric polarisation for an electric field from 0 to 5 kV/cm.

In addition to testing well characterised single crystal samples, the system was also used on thin film samples. The first challenge was finding suitable single crystal samples. The beamline diffractometer geometry is a single crystal system, and although many of the currently produced films show a high degree of texture, few are sufficiently single crystal for these experiments. With IBM as partners in the project we were able to collaborate with several groups making films for their internal PET project, and through a collaboration with Professor Chang-Beom Eom at the University of Wisconsin, we sourced a supply of suitable films.

With piezoelectric thin films come the issue of limited sample size, particularly with respect to sample area. In order to support the applied field without breakdown the sample needs to be pinhole free, and depending on the quality of the film this typically limits the area to less than a square millimetre, and more often less than this. Coupled with the difficulty of making suitable electrical connections to the sample yet still allowing X-ray and interferometer access to the sample, there is also the question of reliably running these experimental films near their operational limits over the extended period required for an X-ray diffraction experiment. These films highlighted a major issue with the use of the system, in that both the X-rays and the interferometer needed to be aligned on the same 200 micron active electrode, i.e. the electrode spot with the applied field. The interferometer alignment was made using optical aids but could in principle be improved with an inline imaging system; the X-ray alignment was more problematical. The X-rays were aligned using an external telescope and X-ray sensitive paper, however it was difficult to confirm this alignment when the sample was moved into the diffraction condition. In practice the confirmation that the X-rays were accessing the active pad was only complete when there was a visible change in the X-ray signal in synchronisation with the applied field. These alignments involved a great deal of time consuming trial and error, and any future developments to the system needs to address this issue.

The films from Wisconsin were PMN-PT since these were the most promising in terms of output for the IBM PET, on a range of substrates: GSO (gallium scandium oxide), silicon and free films on a polymer support membrane. The group at Wisconsin were committed to this collaboration: as well as sending samples they

also sent one or two researchers over for the beamtime, and during one experiment flew a researcher over simply to deliver a sample in time. The group also supplied similar samples to the CNRS group using TEM to study domain motion, and this has led to some fruitful comparisons of the techniques.

As discussed, the measurements of the films have been difficult, particularly because of alignment, but also because the comparison of the interferometer to the X-ray has not been near the 1 to 1 seen for the single crystal sample. The results show that the intrinsic strain as measured by diffraction is around two orders of magnitude smaller than that measured using the interferometer. The major problem with measuring the displacement of piezoelectric thin films using an interferometer is that there is always a large amplification of the displacement due to the bending of the sample. This can be reduced by using a dual beam system to measure the changing in thickness, but even this approach has been questioned in a recent paper published by NPL as a result of these investigations. Use of the free membrane sample was also intended to mitigate this effect, but in separate investigations by NPL the vibratory motion of these samples was much more complex than expected, and the results depended on exactly where the probe is on the sample.

### ***Strain measurements at high frequencies***

A major issue with the method of data acquisition at the XMaS beamline was the difficulty of acquiring data for frequencies at much above 1Hz. The issue is partly a consequence of the time required to acquire a good signal to noise ratio and partly a result of the serial transfer of the XMaS data collection. If for a particular experiment at 10 mHz we need to collect 40 points over a full cycle which will take 100 seconds then by the time we get to 10 Hz we will still need to expose for 100 seconds to get the same signal to noise ratio in the X-rays, but we will collect 40,000 points over 1,000 cycles. Whilst these numbers do not seem that large, the problem is that the XMaS data collection system was not designed to transfer large numbers of data points, so that the transfer of 40,000 data points incurs a time penalty of several minutes. Once this is multiplied by the number of points required to cover an X-ray peak this time penalty becomes prohibitive. Coupled with this is the need to average the data afterwards it meant that data was often not available for assessment until many days after the beamtime was finished.

The choice of data acquisition hardware was limited by the requirement that it needed to be compatible with the rest of the XMaS beamline system and that the ESRF IT support group would need to write code to implement the upgrade. NPL purchased two SP Devices FPGA based data acquisition cards capable of sampling speeds of up to 500MHz, and also contracted SP to write some FPGA averaging software to allow on the fly data reduction. These cards were installed at XMaS and interface code written to control the experiment. In the initial proposal it was thought it would be necessary to access the different bunch modes of the synchrotron, but it was found that this would not be useful for frequencies below 1 MHz. In practice one of the issues has been the difficulty in driving large capacitance samples at high frequencies due to lack of suitable amplifiers. The upgrade as completed made the system much more useable at intermediate frequencies from 1 to 10 kHz, and although in principle it can go to 1 MHz it has not been tested at these frequencies due to inadequate sample availability. Again it was initially thought that the upgrade may yield new insights into domain behaviour at these frequencies but to date nothing unexpected has been seen in the samples tested. Instead the upgrade has highlighted other system aspects not previously seen. For instance the fact that the sample driving amplifier cannot maintain a constant slew rate at higher frequencies displays defects in the displacement signal and this is exactly mirrored in the X-rays. Additionally there were unexpected anomalies in the X-ray data at 100 Hz which appeared and disappeared over time may relate to external vibrations leading to diffractometer misalignment. These were not seen at lower frequencies as they were averaged out over time.

### ***Objective Summary***

This objective was completed successfully: an interferometer was installed on an X-ray beamline for the very first time, and measurements have shown the importance of comparing the change of lattice plane spacing measured by X-ray diffraction with the actual change of length of the sample. The highlights include

- Interferometer installed on diffractometer beamline – this is now a unique facility
- System verified using single crystal samples
- High speed upgrade installed – system turnaround speed increased
- New collaborations developed as a result of the upgraded facility
- System user base increased

**Objective 2: Develop ultra-high spatial resolution (100 nm or less) optical methods of strain measurements using IR-SNOM.**

Two high lateral resolution optical techniques were developed for the characterisation of materials and strain: confocal Raman spectroscopy and near-field infrared microscopy (IR-SNOM), as well as nano-Fourier transform infra-red spectroscopy (FTIR).

**Confocal Raman spectroscopy**

Confocal Raman spectroscopy is a non-destructive laser based technique able to provide information about material composition, crystallinity and strain fields with a lateral resolution of several 100 nm. Far-field methods such as confocal micro-Raman spectroscopy can be used for meso scale characterisation of samples. It can provide information about the spatial chemical and stress distribution in piezoelectric materials and devices. Images are obtained by acquiring spectra from an array of positions and then processing them to reveal the parameter of interest by evaluation of either spectral fingerprints (chemical composition) or splitting and shifts of particular phonon bands (stress). Micro Raman mapping can be performed as in-depth analysis on thin films with layer thicknesses down to 10 nm (depending on the excitation wavelength used). In a lateral arrangement the stress, and therefore the strain distribution can be measured with 300 nm spatial resolution.

Lead zirconate titanate ceramics  $\text{Pb}(\text{Zr}_{1-x}\text{Ti}_x)\text{O}_3$  (PZT) has a regular perovskite structure of type  $\text{ABO}_3$  with a B-cation (Zr, Ti) in the centre of the cube, oxygen ions at the face centres of the cube, and A-ions (Pb) in the cube corners. Generally, a first-order scattering process will give rise to 12 optical modes ( $3 \cdot (r-1)$  where  $r$  is the number of atoms in the unit cell) which are all Raman-active. The 12 phonon modes transform as slightly different irreducible representations, depending on the Zr/Ti ratio and temperature which determines the prevailing solid PZT phase, Figure 3. A LabRam ARAMIS (Horiba Jobin Yvon), a Raman spectrometer, was used for these measurements. The spectrometer was equipped with 4 holographic gratings, 3 excitation lasers (532, 633, 785 nm) and coupled to a confocal microscope (Olympus BX41), and a motorised stage (100 nm resolution) was used for 2-dimensional (x-y) scanning.

Raman spectroscopic measurements were performed on bulk PZT material of nominal composition PZT 52/48 using the Raman spectrometer operated in backscattering mode. The instrument was equipped with a  $600 \text{ mm}^{-1}$  holographic grating, a thermoelectrically-cooled charge-coupled device (CCD) detector and a frequency-doubled Nd:YAG Laser (532 nm) reaching the sample through a 100x objective ( $\text{NA}=0.9$ ). The spectrometer was calibrated with regard to the Raman shift according to ASTM E1840 using compressed microcrystalline sulfur powder as the traceable calibration sample.

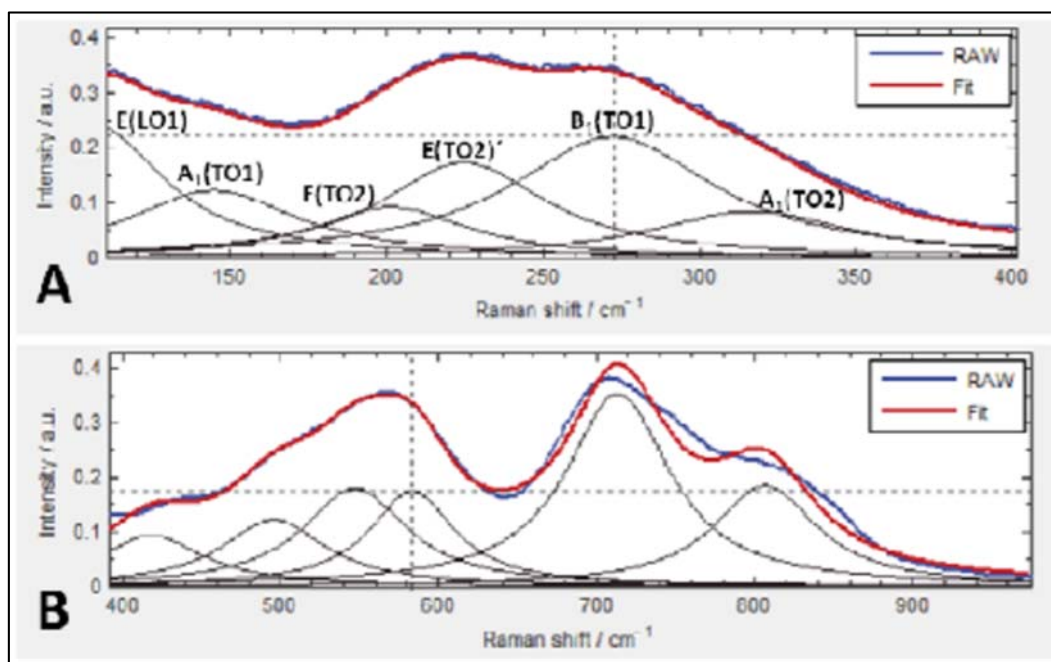


**Figure 3** Raman spectrum from a bulk PZT sample (from  $100 \text{ cm}^{-1}$  to  $1000 \text{ cm}^{-1}$ ) with Lorentzian peak fitting applied.

A proprietary software tool was developed in MATLAB which allowed multi-peak fitting of the Raman modes from the spectral hypercube (i.e. Raman spectrum from each position on the sample in a single file) resulting in either maximum signal intensities or peak positions. Two-dimensional mappings representing the spatially resolved quantity are then easily created from an individual vibrational mode.

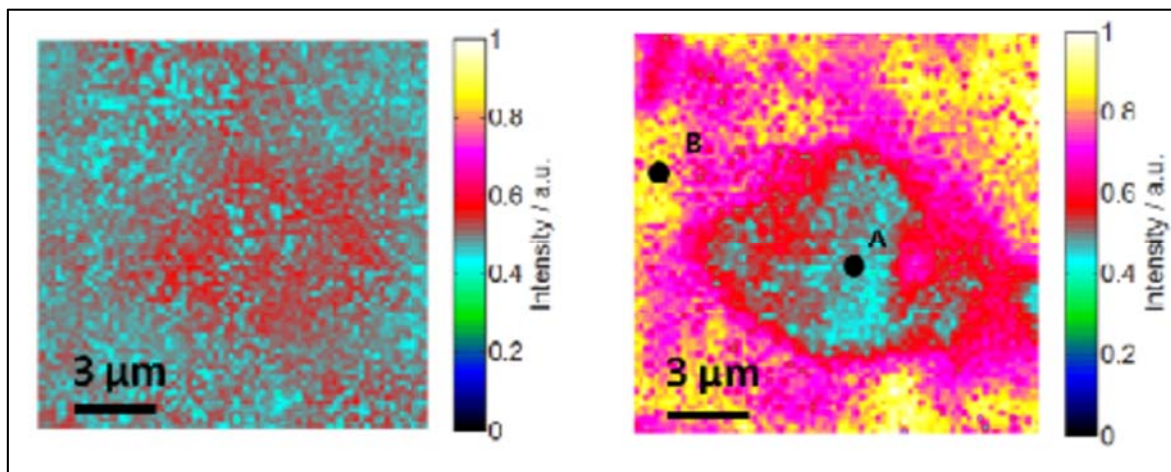


**Figure 4** Intensity distribution of the B1 mode of a bulk PZT sample measured without analyser (left) and in cross-polarised (right) configuration.

The intensity of PZT Raman modes strongly depends on the crystallographic orientation of the sample with respect to the polarisation of the incident laser. In some cases, this could provide a separation of two overlapping bands which particularly holds for the B1 mode around  $270\text{ cm}^{-1}$  and the A1(TO3) modes around  $590\text{ cm}^{-1}$ .

For the B1 mode, this behaviour is clearly demonstrated by the second mapping shown in Figure 4, in which the colour contrast is significantly enhanced compared to the mapping obtained without analyser. A similar effect was found for the intensity distribution of the A1(TO3) mode but in reverse. The intensity distributions show that with increasing intensity of the B mode, the intensity of the A1(TO3) mode decreases. These variations are thought to result from differently oriented domains, rather than different crystal structure or composition. Similar measurements on PZT thin films which had a much finer grain structure did not exhibit any variations which indicate the lateral resolution of the technique is in the sub-micron range but not enough to resolve circa  $\sim 100\text{ nm}$  grains.

#### **Qualification of sub-micro Raman for Strain Determination**

It was not possible to measure changes in samples as a result of piezoelectric strain directly to the low Raman activity of the available piezoelectric materials, so in order to demonstrate the sensitivity of the method the strain produced as a result of a nanoindentation in graphene layers on silicon carbide SiC was investigated. Monolayer graphene epitaxially grown on SiC offers a high potential for electronic device applications similar to piezo ceramics. The material provides excellent properties such as high electron mobility, with the opportunity for wafer-scale fabrication and direct processing on semi-insulating substrates without the need to transfer the graphene to a suitable substrate. Additionally the Raman modes in graphene respond differently on the strain direction, and so Raman spectroscopy is able to distinguish between uniaxial and biaxial strain.

Figure 5 shows the strain around a  $\sim 300\text{ mN}$  nanoindent, mapped using different Raman peaks from the SiC and the graphene. The AFM topography clearly shows the indent close to one of the terrace steps of the graphene layer. There is a large difference in the calculated strain values and the spatial variation between the SiC and the graphene. The maximum value for the SiC is around 0.02, whereas for the graphene it is over 5 times this at 0.1. The main reason for this is due to the low refractive index of SiC in the range of visible light ( $n = 2.2$ ,  $\lambda = 532\text{ nm}$ ). This causes a large depth of the laser focus, which illuminates the substrates across several microns beneath the SiC surface, so the result is an average over this volume. In contrast the thin graphene layer gives very good depth resolution and very high strain sensitivity and the vibrational properties of graphene enable the determination of uniaxial and biaxial strain. Thus, graphene grown on top of “low-Raman-active” materials could be used as ultra-low strain sensor (e.g., on PZT, transparent materials, bulk materials, thin films).

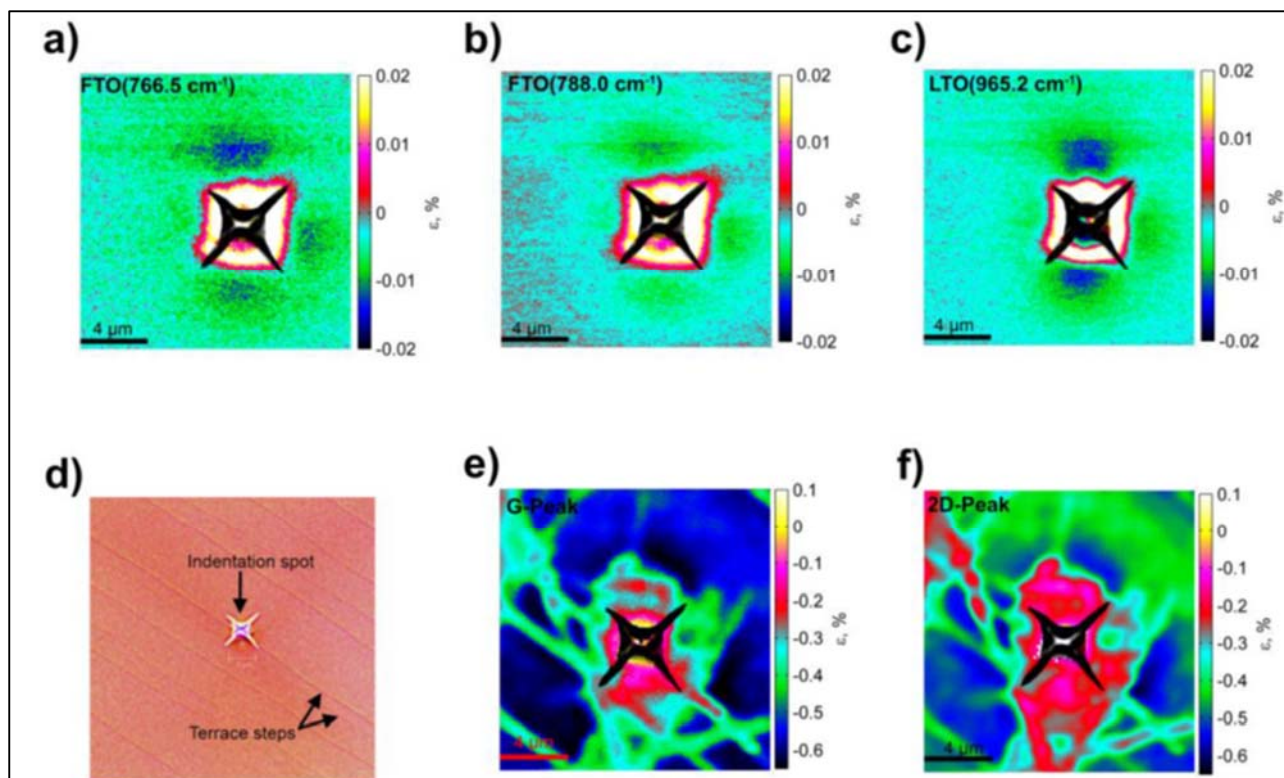


**Figure 5** Strain mapping of 6H-SiC, top row a)-c), AFM topography image d) and epitaxial graphene e), f). The colourbar indicates the residual biaxial strain level.

#### **IR-SNOM and nano-FTIR Spectroscopy: Lateral Sample homogeneity determined by IR-SNOM**

IR spectroscopy is also an optical method and provides complementary chemical information of a sample. In combination with near-field approaches IR-SNOM was able to circumvent the optical diffraction limit, providing a spatial resolution below 40 nm. The group at the PTB low-energy storage ring, used the Metrology Light Source (MLS) as an ultra-broadband IR synchrotron source to increase the accuracy of the technique, taking advantage of the higher source brightness. This enabled the acquisition of the full photon resonance in SiC samples, thus enabling a more accurate determination of the spectral bandshifts than previously possible.

The IR-SNOM system can be regarded as an atomic force microscope (AFM) operated in tapping mode and an asymmetric Michelson interferometer, Figure 6. The highly brilliant and polarised synchrotron radiation is coupled out from the storage ring at a bending magnet and guided to the experiment by several mirrors. The irradiated metal coated AFM tip acts under optimised conditions as an antenna that confines the incident electric field around the tip apex, thus providing a nanoscale light source for near-field investigations. The backscattered radiation from the sample is analysed by the Michelson interferometer consisting of a reference arm and a second arm containing near-field probe and sample. Due to the relatively large size of the focused IR beam (about 80 μm in diameter, see inset **Figure 6**) an illumination of the tip shaft and sample cannot be completely avoided, leading to a strong background contribution. For separating the intensive far-field signal from the relatively weak near-field contribution the interference signal is demodulated at the 2nd, 3rd, and 4th harmonics of the cantilever's oscillation frequency. This provides a signal with strongly decreasing background contribution for higher harmonics ( $n > 1$ ).

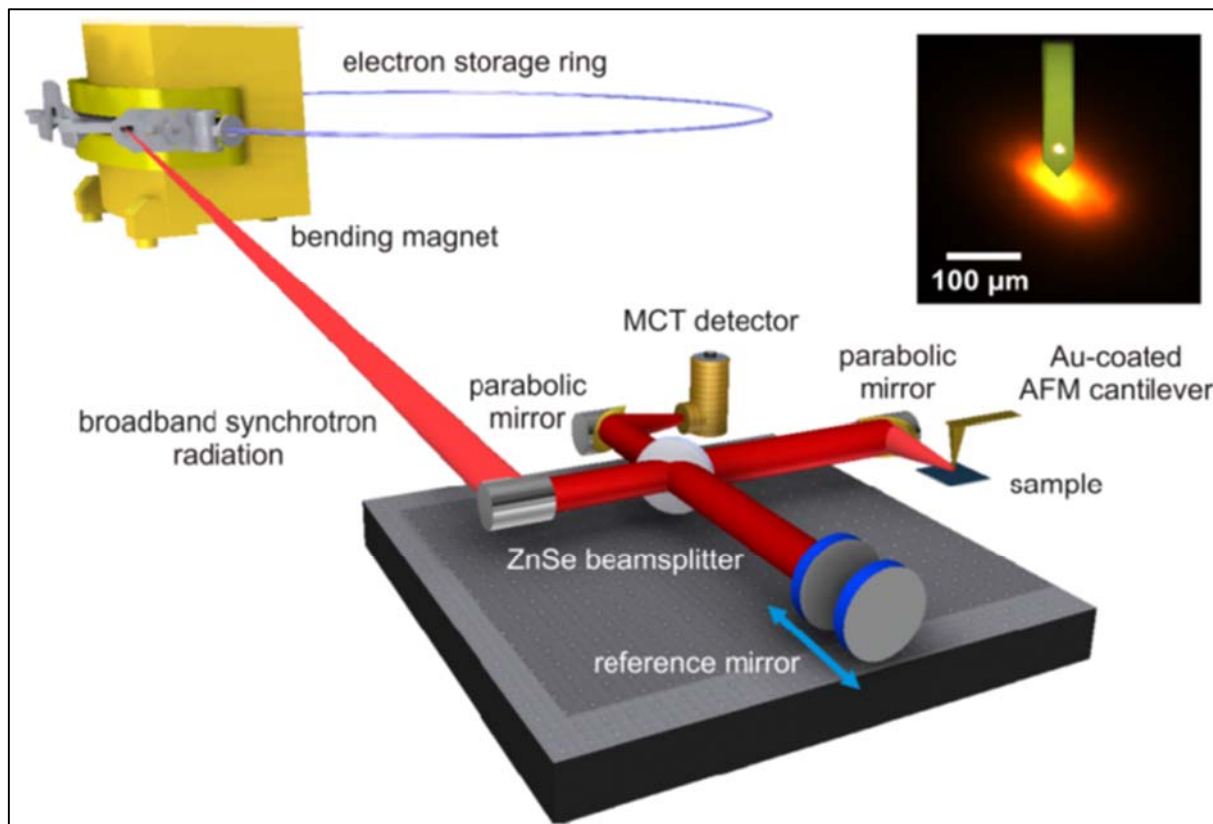


**Figure 6** Schematic diagram of the experimental s-SNOM setup using broadband synchrotron radiation in the IR regime from the electron storage ring MLS. The IR radiation is coupled out at a bending magnet and guided by several mirrors to the experimental setup. The focused IR beam has a diameter of about 80  $\mu\text{m}$  (inset with an optical microscopy image).

To illustrate the lateral resolution of the new nanoimaging setup using synchrotron radiation, near-field imaging experiments were performed on a sample with rectangular  $\text{SiO}_2$  patterns on a Si substrate. The  $\text{SiO}_2$  patterns had an edge length of 1.5  $\mu\text{m}$  x 1.0  $\mu\text{m}$  and a height of about 20 nm. A scan was performed across the  $\text{SiO}_2/\text{Si}$  edge while recording 50 near-field IR spectra over a distance of 1000 nm.

The intensity change during the scan with the wavenumber interval between 962  $\text{cm}^{-1}$  and 1165  $\text{cm}^{-1}$  is shown in Figure 7(a), and the spectral change during the line scan in Figure 7(b). At the  $\text{SiO}_2/\text{Si}$  edge the intensity of the  $\text{SiO}_2$  phonon peak at about 1135  $\text{cm}^{-1}$  decreases to the noise level within a distance of about 40 nm. The results clearly demonstrate that local material composition and properties can be probed with a spatial resolution at the nanoscale using broadband IR synchrotron radiation. The comparison of the results obtained from near-field imaging and spectroscopic nanoimaging show that a spatial resolution around 40 nm can be achieved.

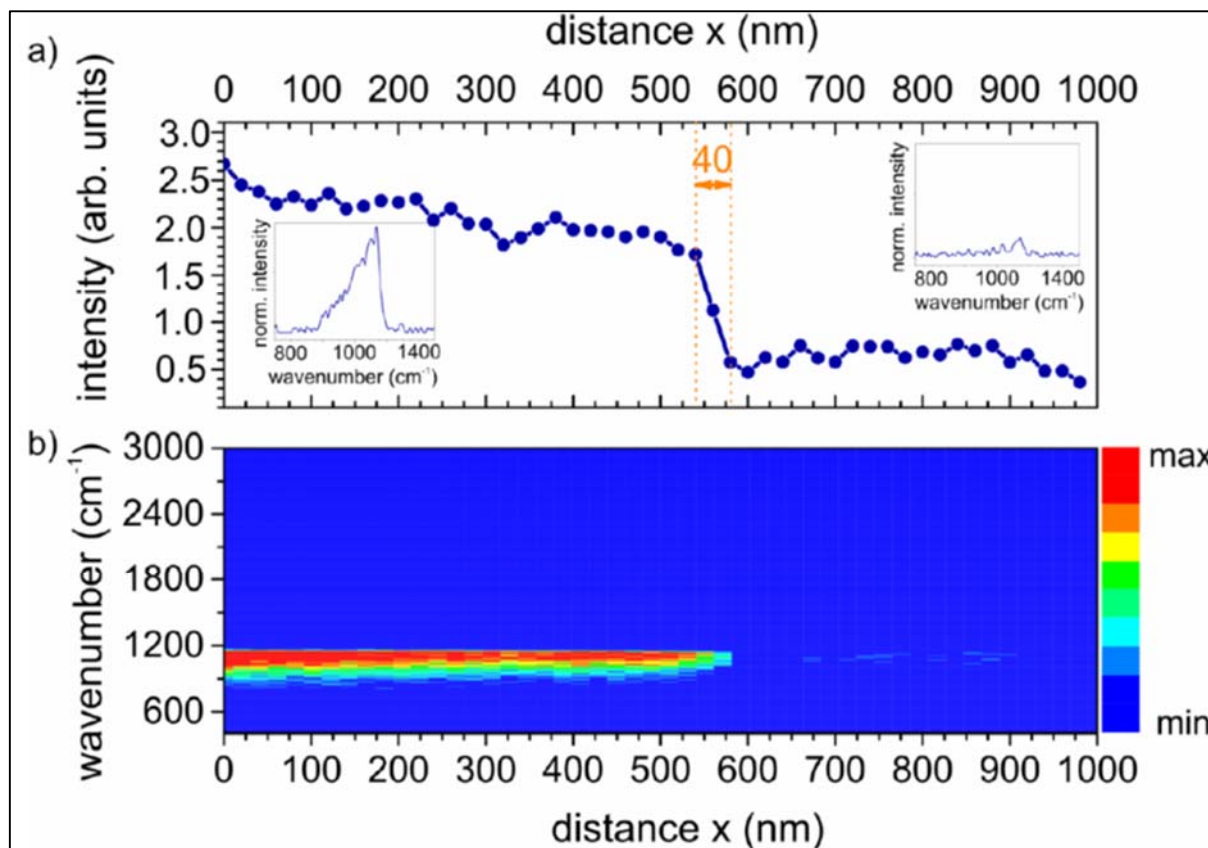


**Figure 7** Intensity (a) and spectroscopic nanoimaging (b) using ultra-broadband IR radiation provided by the electron storage ring MLS. The intensity (S2 spectra) from the Si phonon band at  $1135\text{ cm}^{-1}$  decreases within about 40 nm when performing a scan across a  $\text{SiO}_2/\text{Si}$  edge as documented in the two insets in Figure (a) showing the two nano-FTIR spectra from the line scan recorded from the  $\text{SiO}_2$  and the Si surface. The spectral resolution is about  $6.25\text{ cm}^{-1}$ .

### Objective Summary

The objective was largely completed, and both Confocal Raman spectroscopy and IR-SNOM were used to characterise strain at the nanoscale. However because of the low Raman activity of the available piezoelectric materials it was not possible to measure the strain as a result of the piezoelectric effect, but mapping the strain produced as a result of nanoindentation was realised. Other highlights include:

- Semiconductor materials characterised using synchrotron-based nano-FTIR spectroscopy. Now allows near-field spectroscopic characterisation of nanostructures and thin films by providing information over a much broader wavelength range than with conventional IR radiation sources.
- Results obtained from near-field imaging and spectroscopic nanoimaging show that a spatial resolution around 40 nm can be achieved.
- Adapted storage ring optics for synchrotron-based nano-FTIR spectroscopy. The reduced IR beam size improve the sensitivity and eliminated the need for normalisation of the signal to the ring current by reducing the beam size with decreasing ring current thus keeping the photon flux within the beam unchanged. The additional use of spectral filter increased the sensitivity even further thus enabling successful near-field measurement on organic monolayers.
- Correlative micro-Raman, IR-SNOM and nano-FTIR measurements around nanoindents in graphene-coated SiC samples.
- The highly Raman active graphene layer provides a very high strain sensitivity making it a candidate for an ultra-low strain sensor.
- Development and adaption of fitting routines for evaluation of Raman and nano-FTIR spectra.

**Objective 3: Develop traceable validation of macroscale strain metrology in destructive methods including TEM and novel holographic TEM, to map residual and active (electric field induced) strains.**

TEM offers the ability to image down to the nanoscale, and although chemical and crystallographic information are routine, the techniques to measure and quantify strain are less common. The objective was to apply novel TEM based holographic methods to the measurement of piezoelectric strain. Successful in situ electron microscopy experiments for measuring strain, rely on optimising the process: thin lamella preparation, electrical contacting, observation and analysis.

**Defect and Stress free Lamella production**

The requirement for electron transparency in TEM samples means they have to be as thin as possible (usually 100 nm and thinner). The focussed ion beam (FIB) is a powerful preparation method for preparing thin sections from a selected region of a sample, and the lamella are then thinned by Ga ion bombardment of between 10 and 30 kV. These ions interact with the sample surface giving rise to Ga-implantation and amorphisation. In most cases the damage caused by ion-surface interaction does not impair the sample. However, piezoelectric materials have been shown to be very sensitive to ion irradiation, and prolonged exposure creates irreversible damage. Even for short irradiation times, gallium implantation depths of about 26 nm were measured, which becomes much more crucial for layer thicknesses at the nanoscale. Moreover, this implanted zone is conductive, which is incompatible with the in situ biasing experiments in the TEM. Therefore a strategy was developed for the lamella thinning process to reduce both, the implantation of gallium and the amorphisation. In a systematic study the acceleration voltage of the ion beam was reduced during thinning and the damaged layer thickness of the PZT was checked by TEM. The damaged zone becomes smaller with lowering the acceleration voltage, and in a final NanoMill polishing step the rest of the amorphous material could be removed successfully. Additionally a staircase thinning technique was developed to minimise twisting to obtain a stress-free lamella. Staircase thinning involves reducing the thickness stepwise along the length, Figure 8, and at every step the acceleration voltage is lowered. The staircase supports the stability of the thin lamella and twisting or bending is avoided. The combination of staircase thinning with the reduced accelerating voltage ion beam gives a stress and defect free lamella suitable for TEM imaging.

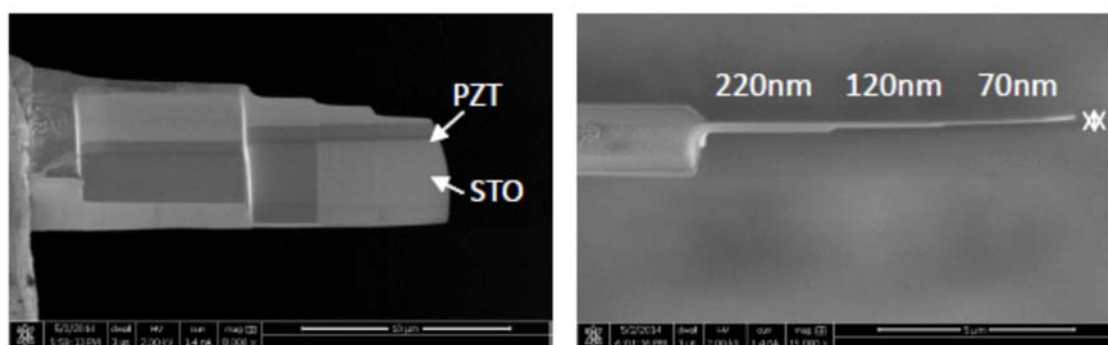


**Figure 8** Staircase thinned PZT TEM sample showing minimal bending as a result of the thicker end support.

**Differential phase-contrast dark-field electron holography (DFEH) for strain mapping**

Electron holography is an interferometric experiment conducted in a transmission electron microscope (TEM) which allows the reconstruction of the phase and the amplitude of a wave. It is used to map electrostatic, magnetic and strain fields at the nanometre scale. Strain characterisation is important to understand the properties of materials, such as the charge carrier's mobility in semiconductors or piezoelectricity in metal oxides, and relate them to fabrication parameters.

There are many different optical configurations for electron holography. The most widespread is the off-axis configuration where a biprism is placed after the specimen. Figure 9(a) illustrates the off-axis configuration for strain mapping in epitaxial thin films, so-called darkfield electron holography (DFEH). The beams diffracted by the substrate are interfered with the beams diffracted by the epitaxial layer. The hologram is recorded using a CCD camera and the phase is numerically reconstructed by Fourier processing. A strain map is then obtained by differentiation of the phase in the direction of the chosen reciprocal lattice vector.

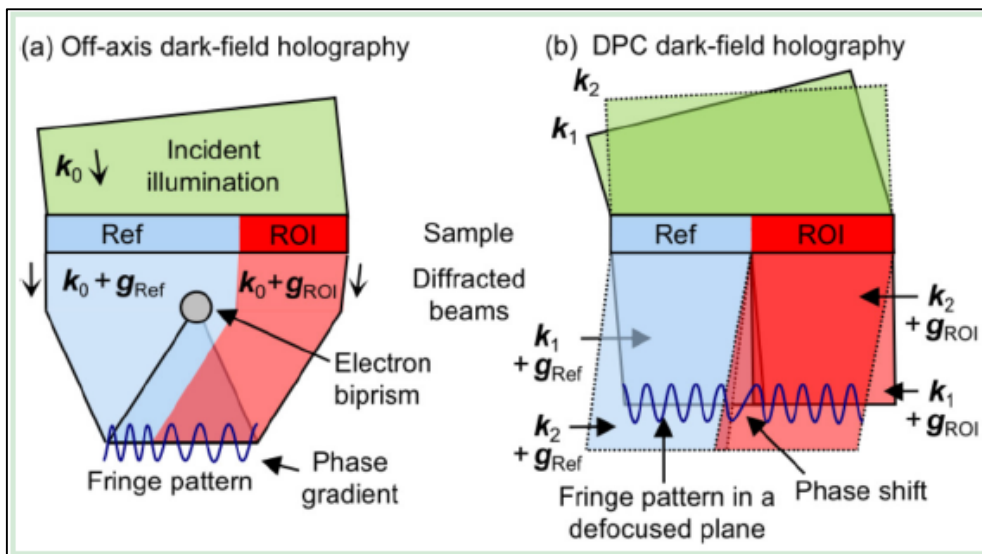


**Figure 9** (a) Dark-field off-axis electron holography. Beams diffracted by a reference region (Ref) are interfered with beams diffracted by a region of interest (ROI) thanks to an electron biprism below the specimen. (b) Differential-phase contrast (DPC) dark-field holography. Two incident beams with a different angle are created by a pre-specimen biprism (not shown here). Beams diffracted by slightly distant regions interfere in a defocused plane.

An alternative darkfield holographic configuration that uses a biprism located before the specimen was developed. This configuration is called differential-phase contrast (DPC). Two incident beams with a different angle are created by the pre-specimen biprism. The hologram is then recorded in a defocused plane where beams diffracted by slightly distant regions of the specimen interfere, Figure 9(b). One advantage of this technique is that the DPC phase reconstructed from the hologram is directly proportional to the strain, providing that the biprism is oriented perpendicularly to the reciprocal lattice vector. Another advantage is that the reference region does not need to be as large as the region of interest.

The technique has been used to investigate the strain in a  $\text{Pb}(\text{Zr}_{0.2}, \text{Ti}_{0.8})\text{O}_3$  thin film epitaxially grown on a  $\text{SrTiO}_3$  substrate. Figure 10(a) is a defocus series of (002) DPC holograms and it contains c- and a-domains (or  $90^\circ$  domains, see representation in Figure 10(c)). The a-domains are needle-shaped and inclined at  $45^\circ$  relative to the STO interface. The DPC phase (Figure 10(b)) is proportional to the growth strain and then increases more rapidly in the c-domains than in the a-domains as a function of the defocus (a being closer to the substrate lattice parameter than c).

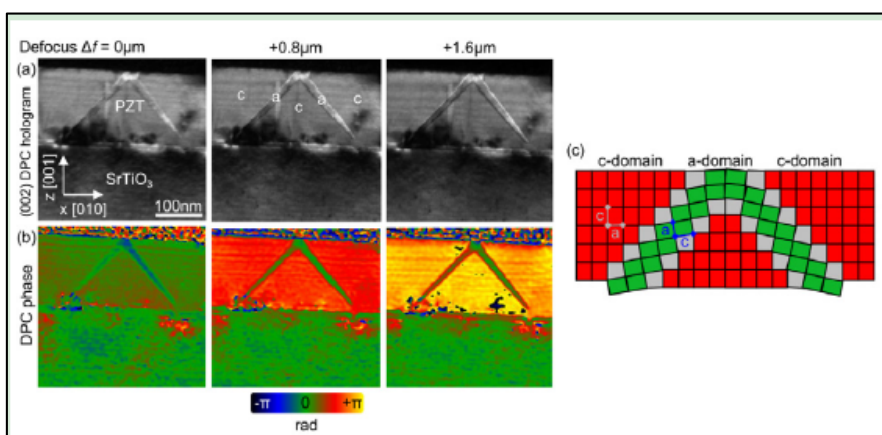


**Figure 10** (a) (002) DPC dark-field electron hologram of a  $\text{Pb}(\text{Zr}_{0.2}, \text{Ti}_{0.8})\text{O}_3$  layer grown on  $\text{SrTiO}_3$  substrate for a range of defocus ( $\Delta f=0$  to  $+1.6 \mu\text{m}$ ). Holograms contain two a-domains with opposite inclination bounded by c-domains. (b) Reconstructed DPC phase image. (c) Representation of the lattice structure.

### *In situ electrical loading*

DFEH is a strain mapping technique, but for application to piezoelectric materials a key objective is to develop methods to apply electric fields to piezoelectric samples inside a TEM. Different methods of applying the field were investigated: the application of a uniform field via an electrode attached to the surface of the film, and the introduction of a charged tip with a nano manipulator. The use of a uniform top electrode did not show any effects of the applied field, presumably due to short circuit leakage paths. Early experiments had used a Hysitron Picoindenter (PI 95) to apply a force to a thin film sample, and so this was used to apply the field directly to the film. Figure 11 shows the nanoindenter probe at the top, with the left hand image is when the tip touches the sample, and the right hand side show the result of applying a 40 V bias, clearly showing domain movement as a result of the applied field. These experiments and others where videos were recorded as the voltage was ramped up and down were largely qualitative. The quantitative mapping of strain during in situ biasing electron holography experiments proved too ambitious. The combined technical problems from straining a film (thus perturbing the diffraction conditions) and electrically biasing (which deflects the electron beam) were the main cause. However, these bottlenecks and others were identified and written up as good practice for follow-on work.

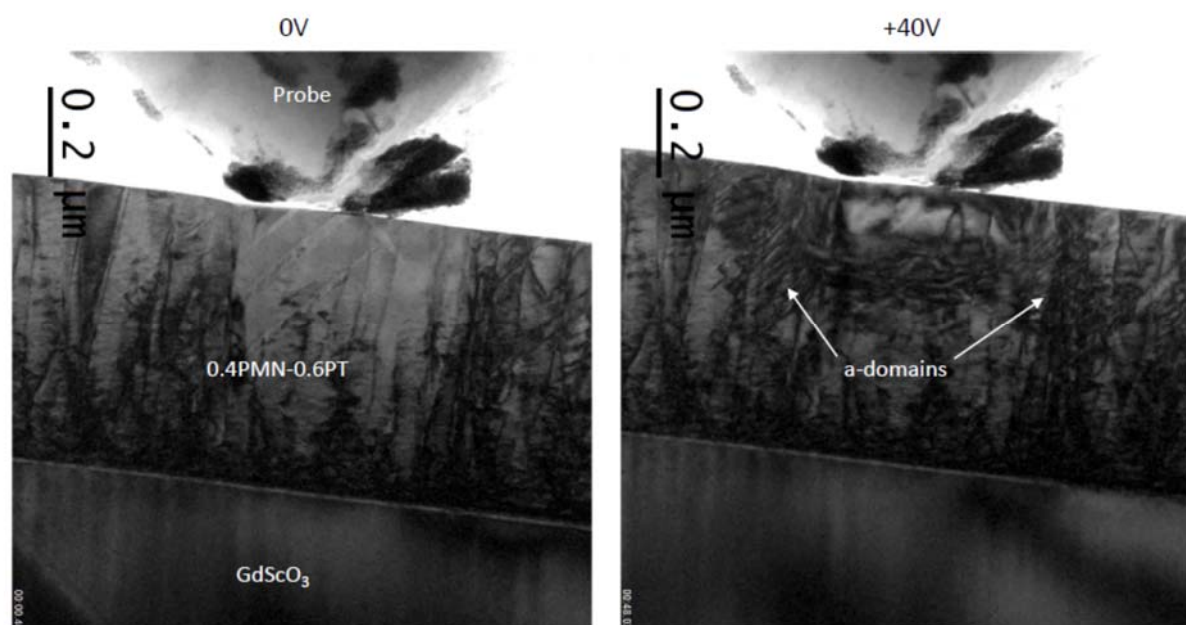


**Figure 11** *In situ* biasing in a TEM of a thinned cross section of PMN-PT piezoelectric film grown on a  $GdScO_4$  substrate. Left hand image, probe in contact, 0 V applied, right hand image with a bias of +40 V.

### **Objective summary**

The technical objectives were largely completed. At the beginning of the project, it was not clear how in situ strain measurements by electron microscopy could be carried out at the nanoscale in piezoelectric thin films. As a result of the work, the way to prepare the specimen, the way to contact the thin lamella electrically, and the way to bias the specimen have all been established. We are now in a position to observe domain wall motion in piezoelectric films under electrical biasing and to see the straining of the film. This is a major step forward to understanding the deformation mechanisms at the nanoscale. In addition, the first quantitative comparisons between experimentally determined strain fields in piezoelectric thin films and finite element modelling have been performed. The highlights of the work include:-

- Sample preparation
  - Influence of lamella thickness, ion beam energy resolved
- Deformation mapping
  - $Pb(Zr,Ti)O_3$ , PMN-PT,  $BaTiO_3$  grown on oxide or Si substrate
  - Strain gradients → Flexoelectricity

- In situ biasing
  - Domain switching with and without top electrode
  - Difficult to perform in situ and holography simultaneously
- Electron holography developments
  - Two new techniques developed for strain analysis
- STEM imaging and polarisation mapping
  - Reconstruct strain and polarisation in real space and reciprocal space

#### Objective 4: Develop multiphysics materials modelling

This objective was to provide a theoretical insight into the origin and control of strain in nano-scaled piezo- and ferroelectric materials, both to support the experimental work in this project and to provide tools for future device development. Most of the modelling work related to piezoelectric materials is currently at the mesoscale, using finite element analysis (FEA) or analytical methods. The focus here was to develop atomistic models, using first principles i.e. ab initio simulation methods that would enable the exploration of different material architectures and structures.

#### Force Field Developments in PZT modelling

Much of the work was carried out at NPL collaborating with partners at UCL to develop a robust approach for predicting the properties of large-scale piezoelectric systems based on modelling the force field.

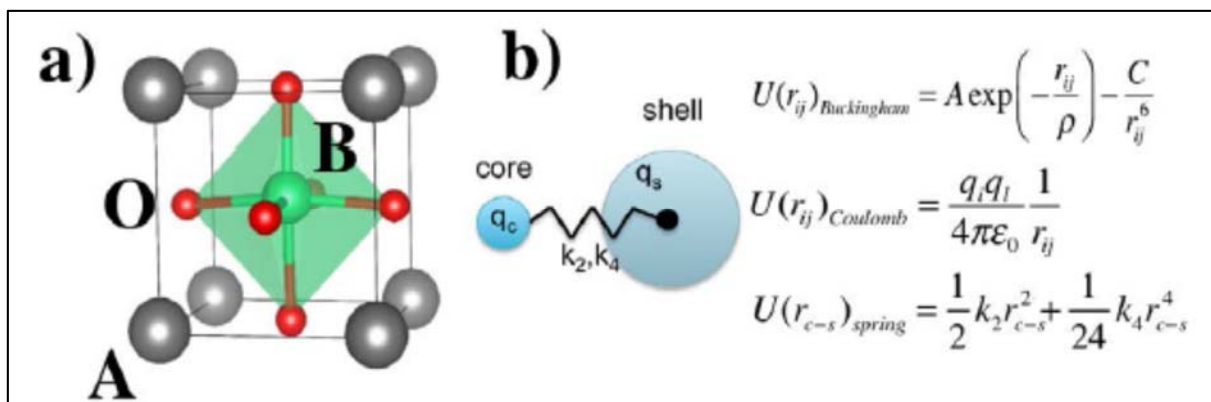


**Figure 12** (a) Structural unit of ABO<sub>3</sub> perovskite. (b) Shell model represents ion that consists of two particles, a core and a shell standing for the atomic nucleus and electron shell, respectively. Shell model is parametrised with three types of interactions: long-range  $U_{Coulomb}(r_{ij})$ , short-range  $U_{Buckingham}(r_{ij})$ , and core-shell  $U_{spring}(r_{c-s})$  spring potentials.

PZT belongs to a class of disordered solid solution perovskite materials A(BB')O<sub>3</sub>, where the disorder is caused by the random arrangement of B cations, i.e. Ti and Zr, Figure 12(a). Relating the origin of compositional phase transitions and morphotropic phase boundaries (MPBs) to properties of individual atoms is crucial for understanding the way variations in atomic composition affect material properties. Such microscopic understanding is needed for the design of better materials and is most naturally obtained from calculations based on first principles. Such ab initio calculations, based on density functional theory (DFT) have, over the years, been extensively applied to various ferroelectric materials. They have provided a fundamental insight into the origin of ferroelectricity, as well as the behaviour of domain walls, grain boundaries, and interfacial phenomena.

Although the DFT method is a powerful tool, modelling PZT (as well as more general solid solution systems) from a first principles perspective can be challenging as it is only possible to study small system sizes with this method. The quenched disorder in the B-cation arrangement creates a “statistical gap” between small, DFT-accessible super-cells and the real material. The long-range Coulomb interactions of the charged ions in the system enable long-range structural correlations, which are indirectly seen via diffraction experiments, and these display a variety of phase distortions away from the high-symmetry positions which cannot be modelled in small systems. Interatomic force fields, based on the shell model, can be used to bridge the statistical gap

as these force fields can be used for atomic simulations of large systems that capture the full disorder of the real materials.

Ferroelectricity originates from the delicate balance between long-range Coulomb and short-range repulsive interactions, and the shell model can explicitly represent both. Moreover, the shell model is capable of describing ionic polarisability by assuming the existence of two hypothetical particles – a core and a shell – which represent the atomic nucleus and electron shell respectively, Figure 12b.

The objective is to use this shell model to develop a robust interatomic force field for PZT that reproduces its phase stability, structural and ferroelectric properties, as well as details of the phase diagram. To this end, the parameters of the shell model functions were carefully fitted so that the force field (FF) correctly reproduced the fundamental properties of the  $\text{PbTiO}_3$ ,  $\text{PbZrO}_3$  and the lowest energy  $P4mm$  ordered phase of  $\text{Pb}(\text{Zr}_{0.5}\text{Ti}_{0.5})\text{O}_3$ , including phase stability, crystal structures, elastic constants, and effective charges derived from DFT calculations. The FF developed accurately reproduces the details of the PZT phase diagram in good agreement with experiment. Indeed, the FF fully reproduces the tetragonal structure of  $\text{PbTiO}_3$  in PZT at  $x=100\%$ . With the decrease of Ti-content ( $0.5 < x < 1$ ) the structure remains tetragonal. Meanwhile, at the other end of the PZT phase diagram ( $x=0\%$ ), the FF also reproduces the antiferroelectric structure of  $\text{PbZrO}_3$ , and supports rhombohedral structure on the zirconium-rich side, Figure 13. Calculations of the structure and stability of domain walls in PZT produce excellent agreement with properties predicted from ab initio calculations, and the FF predicts very sharp domain walls of about 8 Å that are also in good agreement with TEM images.

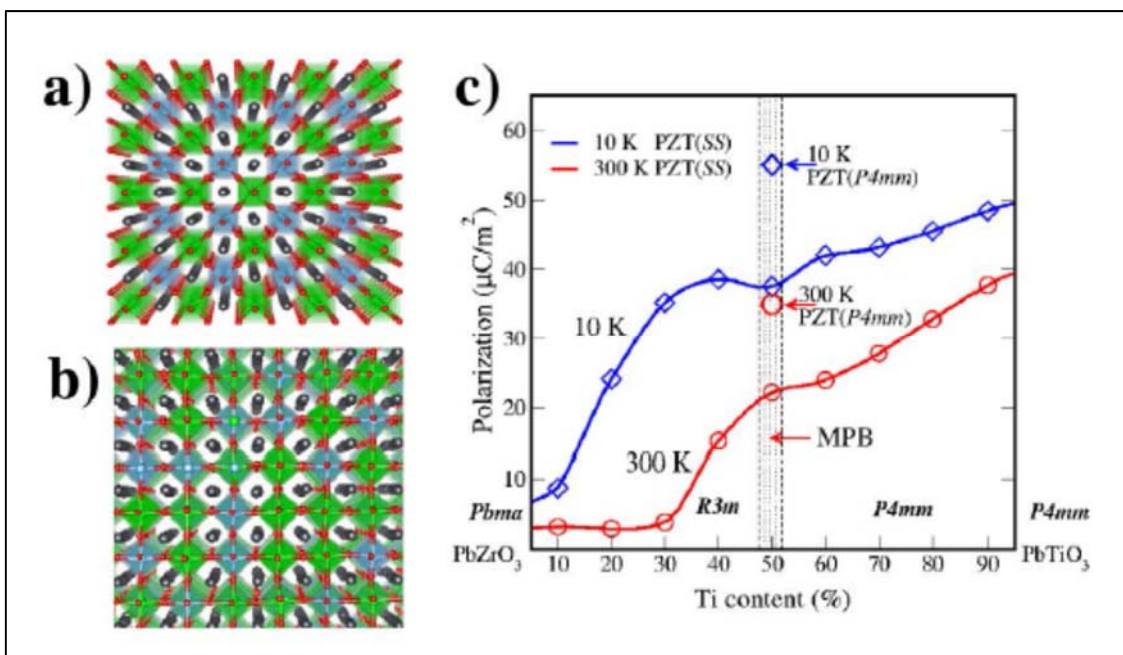


**Figure 13** (a) Phase diagram of  $\text{Pb}(\text{Zr}_x\text{Ti}_{1-x})\text{O}_3$  reproduced by shell-model force field. At  $x=0\%$  antiferroelectric  $\text{Pbma}$  phase is supported, while at another end ( $x=100\%$ )  $P4mm$  phase of  $\text{PbTiO}_3$  is supported. At low Ti-content FF reproduces rhombohedral phase, while at high Ti-content tetragonal phase is prevalent.

#### FEA and analytical modelling for experimental support

As well as developing ab initio models to aid deeper understanding of materials and device behaviour, more mesoscale modelling techniques such as FEA and analytical models were developed to aid experimental design and understanding. This was particularly true for the modelling of thin films, where there were several successes key to understanding how piezoelectric thin films behave on silicon substrates. Many experimental techniques to measure the piezoelectric activity of thin films rely on measuring the change of thickness of a sample and the modelling has helped the understanding of how to make these measurements reliably, where the governing factor is the size of the top electrode on the piezoelectric film, Figure 14.

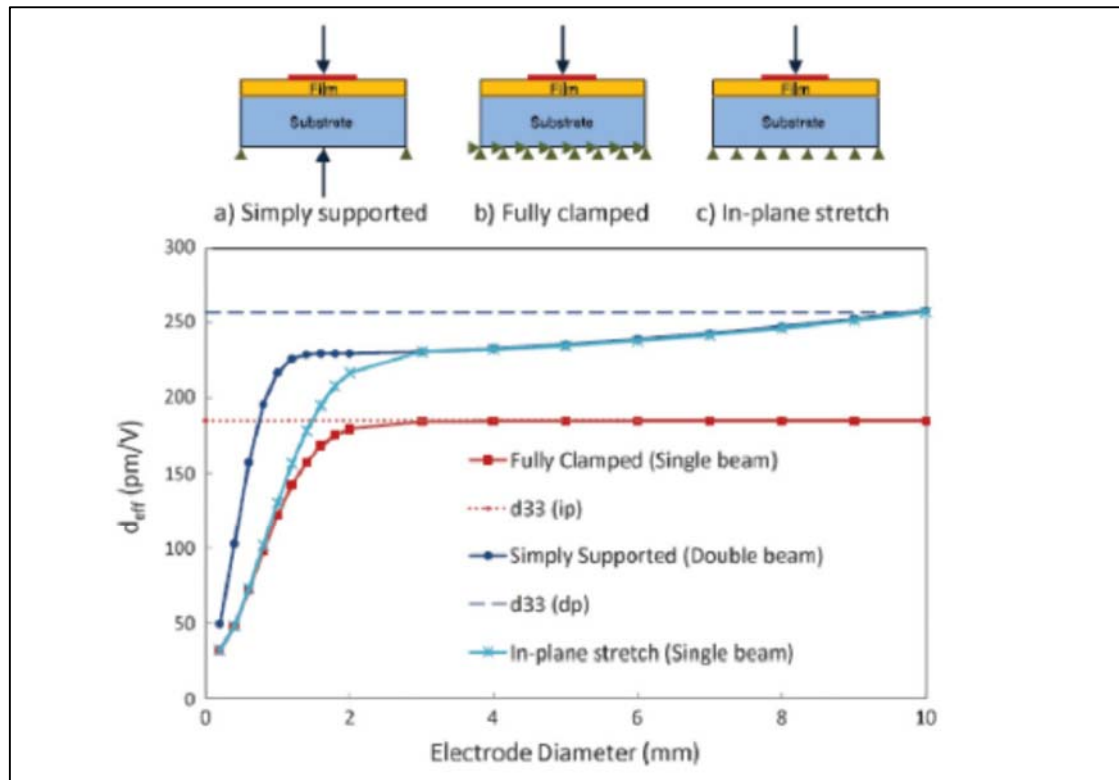


**Figure 14** FEA simulations of change in sample thickness along with schematics of the representations of the simply supported (a), fully clamped (b), and in-plane stretch case (c).

### Objective Summary

The ab-initio modelling tools developed showed significant success and widely extend the applicable range of atomic-level simulations of ferroelectrics based on the shell model potential. Further molecular dynamics simulations based on the shell model force field provide atomic level insight into the domain wall kinetics in a multi-domain system under external stimuli (such as strain and/or electric field). The ability to predict domain wall formation and their dynamics is central to design at the nanoscale level, and such research takes us a long way towards accomplishing this important goal. The mesoscale modelling also yielded key insights into understanding not only experimental results but also as an aid to future device design.

### Objective 5: Extend the use of Digital Image Correlation processing to nano-scale functional atomic force microscopy, SEM and other strain mapping images.

Digital Image Correlation (DIC) is an important technique to visualise how samples behave under stress. Developed in the 1980s as a way to visualise local in-plane deformations of an object, DIC relies on comparing two images of the sample: one taken under normal conditions (a reference image) and the other when influenced by some external stimulus (a distorted image). The aim of the method is to detect very small changes in sample displacements and strains caused by the external stimulus and then to compare it to sample deformation as predicted by some analytical relation or numerical model. The objective within this project was to visualise local displacements in a material as a result of the piezoelectric effect. Generally the DIC method has been used with optical images, but in principle any digital image can serve as an input. This means that the technique can be applied to data obtained from atomic force microscopes (AFM) as well as most types of electron microscopes.

CMI developed a set of software tools for DIC processing as part of their open source image analysis software Gwyddion, (<http://gwyddion.net>). The main tool is a crosscorrelation module, and using this module the shifts in the x and y axes can be calculated from the reference and distorted images. The module is a part of the standard Gwyddion installation and so is now available to the wide community of Gwyddion users. **Figure 15** shows a screenshot of the software being used on a set of the Society for Experimental Mechanics DIC

challenge images, a set of standard images designed to test DIC software. At present the capability in Gwyddion is one of the few DIC solutions available in the public domain. The software was used to measure piezoelectric strain in a number of samples, and was particularly successful when using optical images where there was good signal to noise.

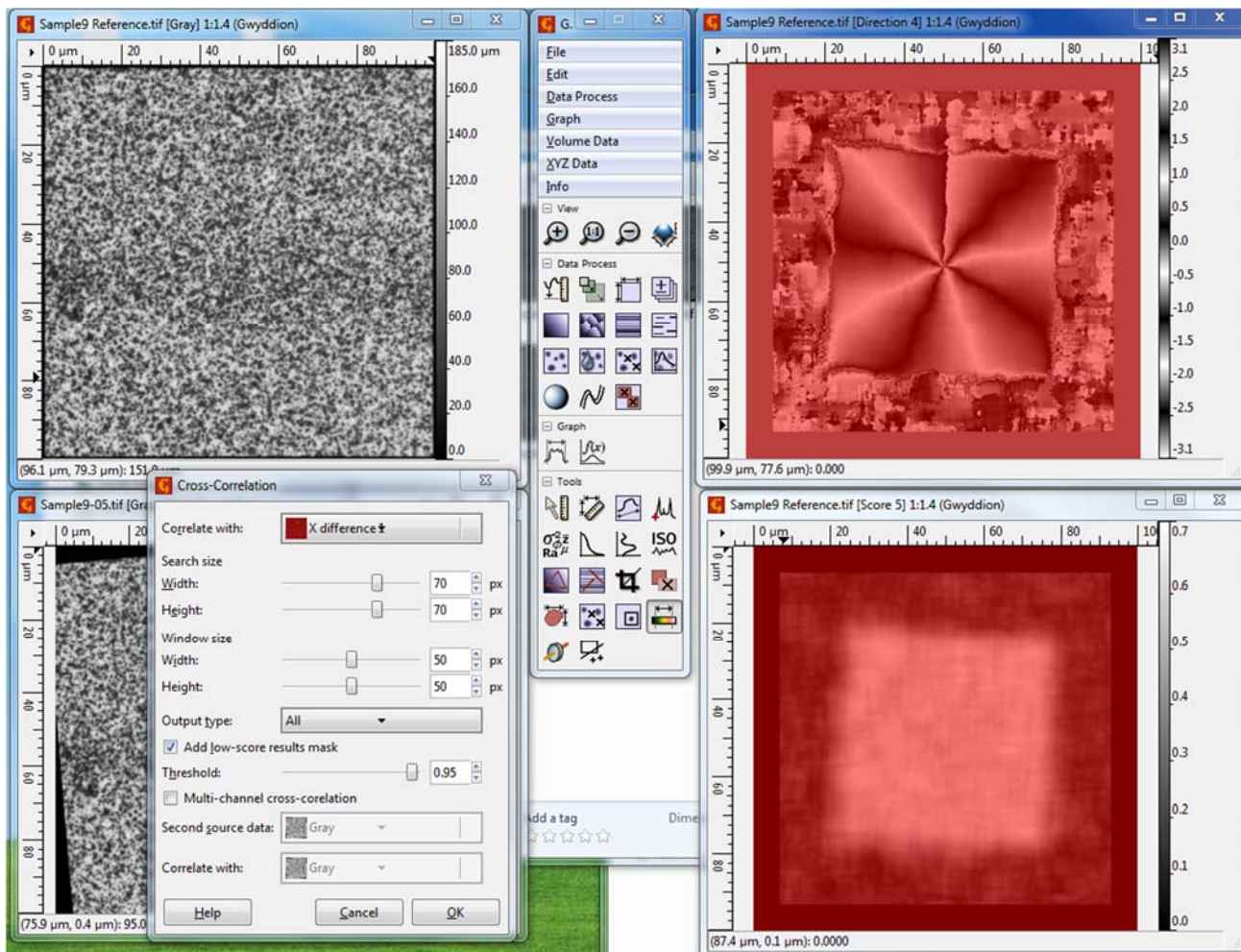


**Figure 15** Gwyddion open source AFM image processing software, showing the cross correlation module used for DIC. The analysis is on an SEM-DIC challenge test image for rotation. The results in top right corner in red show the x-shift of the image, and the bottom corner shows the confidence level in the result.

For AFM images, although it was possible to run the DIC analysis to see the effect of piezoelectric strain, the low signal to noise resulted in poor quality results. One of the problems is that the with and without voltage applied images should be identical and with typical AFM images taking a few minutes, drift was a constant problem. To overcome this the slow scan axis of the microscope was interleaved so that each line had alternately zero and positive voltage applied. In the SEM the signal to noise was less of an issue but generally the DIC highlighted defects in the microscope scanning system that were greater than expected from the piezoelectric strain. Figure 16 shows two DIC images where there are diagonal stripes across the x shift image. The frequency of these bands doubles as the scan speed halves suggesting that it is an artefact rather than the piezoelectric effect. In this case it was found to be related to poor grounding issues associated with feeding through external bias voltage into the SEM chamber, which was reduced when a floating power supply was used. In fact the majority of the SEM based DIC work was devoted to minimising these artefacts and using DIC to characterise SEM issues.

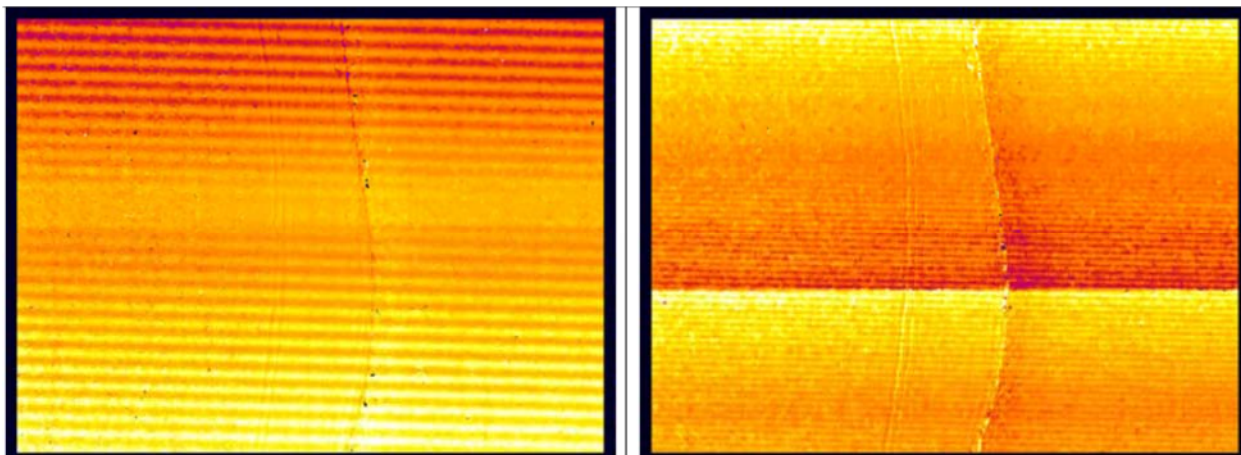


**Figure 16** DIC x shift images of a PZT sample with an applied voltage. The wavy vertical line marks the boundary between the top electrode and bare PZT. The image on the left was taken at a scan speed of 40 seconds, and the right hand image at 80 seconds. The horizontal stripes are an artefact produced by inadequate shielding.

### Objective Summary

Within this objective the use of Digital Image Correlation was extended to nanoscale functional AFM and SEM to characterise piezoelectric strains. Optical imaging DIC was successfully demonstrated, including measuring shear strain, however the SEM based imaging DIC revealed technique limiting artefacts. In fact these artefacts had been noted in other studies outside this project, however the work here concentrated on successfully identifying their cause and developed ways to minimise them. An open source module for performing DIC analysis was developed as part of Gwyddion.

## 4 Actual and potential impact

A project website was setup on the Piezo Institute website as well as mirroring much of the content on the XMaS beamline website. Seven editions of the project newsletter were produced, with contributions from all of the project partners and stakeholders, to keep people updated on the project progress. These were emailed to stakeholders and made available via the project webpage. As well as the technical progress, each issue also included an interview with one of the project stakeholders to gauge their opinions, as well as their latest developments in their field. A series of webinars were developed for the website, detailing a specific project work-package. A number of high profile articles were published in the trade press, initially to promote the beginning of the project with coverage in the New Scientist, The Daily Telegraph and Physics World. Towards the end, to coincide with a growing interest in energy consumption of server farms, several articles promoting the low power consumption possibilities of the PET transistor work were published ([www.computerweekly.com/opinion/Reinstating-Moores-Law-a-next-gen-transistor-for-mobile-technology](http://www.computerweekly.com/opinion/Reinstating-Moores-Law-a-next-gen-transistor-for-mobile-technology)). In all, over 30 short articles highlighting the project were published in the trade press and websites.

The project team gave over 50 presentations/ tutorials at various conferences and symposia. The consortium members were involved in organising a session at the E-MRS Spring Meeting 2014 - Symposium H: ALTECH 2014 "Analytical Techniques for Precise Characterization of Nano Materials", where seven of the presentations were given by consortium members. In July 2015, NPL hosted a two day conference, UK Ferroelectrics 2015, where Carlo Vecchini gave an invited presentation, "In situ Dynamic Electrical and Structural Measurements of Functional Materials" covering the X-ray diffraction work developed within the Nanostrain project. The high profile of the work led to NPL and XMaS joining forces with the Advanced Photon Source (APS), to run a workshop couched under the APS annual user meeting to discuss the future of in situ, in operando sample environments needed for the next generation of synchrotron X-ray experiments.

There were several other collaborations that came about as a result of the work at large scale facilities such as XMaS at ESRF, that were not explicitly envisaged at the beginning but nevertheless contribute to the skills and understanding needed to do this work. A collaboration with a researcher, Gareth Nisbet, at Diamond Light Source looked at using a novel technique, Diffuse Multiple Scattering (DMS), on this class of material. DMS uses a large area detector to collect 2D patterns similar to Kikuchi lines and these patterns give a unique

fingerprint to the strain in the sample. The collaboration initially involved some beamtime at ESRF with ULiv, NPL, and Diamond, but later separate beamtime was applied for and won at Diamond. Work is ongoing to produce a publication from this work. A second collaboration came at the ISIS Neutron source at the Rutherford Appleton Laboratory with the Wish magnetic beamline. Wish is a long-wavelength diffractometer primarily designed for powder diffraction at long d-spacing in magnetic and large unit cell systems. The collaboration included installation of an in situ applied field and charge measurement capability as installed at ESRF and then some initial experiments on novel multiferroic samples provided by the Queen Mary University.

The project led to the publication of 14 scientific papers in peer reviewed journals, with several more still in the pipeline. The work established good practice in several areas, some hosted on the XMaS beamline site, giving practical information about the equipment and how to operate it ([http://www2.warwick.ac.uk/fac/cross\\_fac/xmas/other\\_projects/nanostrainproject/](http://www2.warwick.ac.uk/fac/cross_fac/xmas/other_projects/nanostrainproject/) and [http://www2.warwick.ac.uk/fac/cross\\_fac/xmas/xmas\\_offline/electrical\\_measurements/](http://www2.warwick.ac.uk/fac/cross_fac/xmas/xmas_offline/electrical_measurements/)).

Although the Nanostrain activity was largely pre standards, the results on evaluating measurement best practice were fed into VAMAS, who develop the standards for advanced materials. Participation in this group led to the development and publication of the ISO/TC 206 standard (NP1013) on high strain measurements of piezoelectrics.

The outcomes of the project have led to the development of some unique and world leading facilities to characterise piezoelectric devices, which are now available for use by researchers worldwide.

- The in situ Nanostrain measurement facilities developed by NPL and the XMaS beamline (ULiv) is now fully operational providing both academic and industrial scientific community (X-ray and offline) access, to both high brightness Synchrotron and off line Lab source system. This has led to several collaborations with high profile research groups at the University of Wisconsin, and Penn State, and to increased requests for beam time on the system.
- For the in-plane DIC Nanostrain procedures developed under this project the community now has access to Multichannel DIC as a module for open source software Gwyddion (see <http://gwyddion.net>).
- The development of ab initio modelling capabilities for the origin and control of strain in nano-scaled piezo- and ferroelectric materials, mostly at NPL, resulted in requests to access the expertise in modelling oxide films from a company developing dielectric coatings.
- A new analytical capability, synchrotron-based nano-FTIR spectroscopy was established at the PTB low-energy storage ring, the MLS, and is available for both academic and industrial users.

The project also helped to train young scientists working in this field, both within and beyond the consortium. The establishment of these new capabilities were the scientific and technical objective of the project and will support industry to develop the next generation of processors.

The partners involved in the Nanostrain project will continue their collaboration, and further develop the expertise and capabilities started in Nanostrain in two related follow on European projects. The first of these is the Horizon 2020 project PETMEM (Piezoelectronic Transduction Memory Device). This is a European partnership of universities, research institutions, SMEs and businesses including IBM, SolMateS and aixACCT that aims to build a proof of concept prototype PET memory device and to develop the tools and processes to allow other people to design with and make piezoelectric transistor technology. Alongside PETMEM is the EMPIR project 16ENG06 ADVENT, "Metrology for advanced energy-saving technology in next-generation electronics applications". The consortium includes some of the Nanostrain partners such as NPL and PTB. The ADVENT project will look at low-powered high efficiency microelectronics, with the aim of developing the suite of metrology needed for industry to develop and to use low powered materials, electronics, components and systems.

In the longer term the development of the new technologies from this project will help stimulate innovation in the microelectronics industry, with consequential economic benefits in ensuring strong European participation in the growth of the nanotechnology market. Additional environmental benefits arise from the reduced energy requirements of electronic devices utilising this technology, and therefore increased battery life of devices. Better sensing and electronic technologies will also increase the speed of computers.

## 5 Website address and contact details

<http://www.piezoinstitute.com/resources/emrp-nanostrain/>

[http://www2.warwick.ac.uk/fac/cross\\_fac/xmas/other\\_projects/nanostrainproject](http://www2.warwick.ac.uk/fac/cross_fac/xmas/other_projects/nanostrainproject)

[mark.stewart@npl.co.uk](mailto:mark.stewart@npl.co.uk)

## 6 List of publications

1. L. N. McCartney, L. Wright, M. G. Cain, J. Crain, G. J. Martyna, and D. M. Newns "Methods for determining piezoelectric properties of thin epitaxial films: Theoretical foundations", *Jnl. Appl. Physics*, 116, 014104 (2014).
2. M. Hytch and A. M. Minor "Observing and measuring strain in nanostructures and devices with transmission electron microscopy", *MRS Bulletin*, 39, Feb 2014, 138-146.
3. N. Wollschläger, W. Österle and M. Stewart "A Systematic Study of Ga<sup>+</sup> Implantation in a PZT Film during Focused Ion Beam Micro-machining", *Physica Status Solidi*, (c), 12, 2015, 314-317
4. M. Stewart, S. Lepadatu, L. N. McCartney, M. G. Cain, L. Wright, J. Crain, D. M. Newns, and G. J. Martyna, "Electrode size and boundary condition independent measurement of the effective piezoelectric coefficient of thin films", *APL Materials*, 3, 026103 (2015)
5. N. Jalali, P. Woolliams, M. Stewart, P. M. Weaver, M. G. Cain, S. Dunn and J. Briscoe, "Improved performance of p-n junction-based ZnO nanogenerators through CuSCN-passivation of ZnO nanorods", *Journal of Materials Chemistry A*, 2, 2014, 10945-10951.
6. N. Jalali, J. Briscoe, Y. Z. Tan, P. Woolliams, M. S., P. M. Weaver, M. G. Cain and S. Dunn, "ZnO Nanorod Surface Modification With PDDA/PSS Bi-Layer Assembly For Performance Improvement Of ZnO Piezoelectric Energy Harvesting Devices", *EMRS Conference Proceedings* (2014), *J. Sol-Gel Sci. Technol.* 73, 554 (2015).
7. T. Denneulin, F. Houdellier and M.J. Hytch "Differential phase-contrast dark-field electron holography for strain mapping". *Ultramicroscopy* 160, 98-109 (2016).
8. C. Vecchini, P. Thompson, M. Stewart, A. Muniz-Piniella, S. R. C. McMitchell, J. Wooldridge, S. Lepadatu, L. Bouchenoire, S. Brown, D. Wermeille, O. Bikondoa, C. A. Lucas, T. Hase, M. Lesourd, D. Dontsov and M. G. Cain "Simultaneous dynamic electrical and structural measurements of functional materials", *Review of Scientific Instruments*, 86, 103901, (2015).
9. T. Denneulin and M. J. Hytch "Four-wave dark-field electron holography for imaging strain fields", *J. Phys. D: Appl. Phys.* 49, 244003 (2016).
10. O. Gindele, A. Kimmel, M. Cain and D. Duffy, "Shell model force field for PZT", *J. Phys. Chem. C* 119, 17784 (2015).
11. J. Chapman, A. V. Kimmel and D. M. Duffy, "Novel high-temperature ferroelectric domain morphology in PbTiO<sub>3</sub> ultrathin films" *Phys. Chem. Chem. Phys.* 2017, 19, 4243-4250.
12. A. Bogdanov, A. Mysovsky, C. J. Pickard and A. V. Kimmel, "Modelling the structure of Zr-rich Pb (Zr<sub>1-x</sub>Ti<sub>x</sub>) O<sub>3</sub>, x = 0.4 by a multiphase approach", *Phys. Chem. Chem. Phys.*, 2016, 18, 28316-28324.
13. A. Kimmel, P. Sushko, "Mechanism of formation of chemical bonds and defects at oxide/ferroelectric interfaces", *J. Phys. Cond. Matt.*, 24 (4) 475006 (2015).
14. T. Denneulin, W. Maeng, C.-B. Oem, and M. J. Hytch, "Lattice reorientation in tetragonal PMN-PT thin film induced by focused ion beam preparation for transmission electron microscopy", *J. Appl. Phys.* 121, 055302 (2017).